

Long-Range Wireless Interrogation of Passive Humidity Sensors Using Van-Atta Cross-Polarization Effect and Different Beam Scanning Technique

Dominique Henry, Jimmy Hester, Hervé Aubert, Patrick Pons, Manos M. Tentzeris

► **To cite this version:**

Dominique Henry, Jimmy Hester, Hervé Aubert, Patrick Pons, Manos M. Tentzeris. Long-Range Wireless Interrogation of Passive Humidity Sensors Using Van-Atta Cross-Polarization Effect and Different Beam Scanning Technique. IEEE Transactions on Microwave Theory and Techniques, Institute of Electrical and Electronics Engineers, 2017, 65 (12), pp.5345-5354. 10.1109/TMTT.2017.2769055 . hal-01710107

HAL Id: hal-01710107

<https://hal.laas.fr/hal-01710107>

Submitted on 15 Feb 2018

HAL is a multi-disciplinary open access archive for the deposit and dissemination of scientific research documents, whether they are published or not. The documents may come from teaching and research institutions in France or abroad, or from public or private research centers.

L'archive ouverte pluridisciplinaire **HAL**, est destinée au dépôt et à la diffusion de documents scientifiques de niveau recherche, publiés ou non, émanant des établissements d'enseignement et de recherche français ou étrangers, des laboratoires publics ou privés.

Long Range Wireless Interrogation of Passive Humidity Sensors using Van-Atta Cross-Polarization Effect and Different Beam Scanning Techniques

Dominique Henry, Jimmy G.D. Hester, Hervé Aubert, Patrick Pons and Manos M. Tentzeris

Abstract—This paper presents a method for the remote interrogation of batteryless humidity sensors based on statistical estimations and three-dimensional beam scanning techniques. As a proof-of-concept demonstration, a Van-Atta reflectarray sensor is interrogated with a 24 GHz Frequency-Modulated Continuous-Wave transceiver at various reading ranges. The extension of the proposed approach to passive or moving sensors is reported and measurement results are discussed. The relative humidity is derived from the statistical analysis of multidimensional radar echoes, while method is proposed to detect the sensor among clutter without knowing its exact position. Moreover it is demonstrated that the cross-polarization effect of the Van-Atta reflectarray combined with the 3D beam scanning technique allows the indoor measurement of the relative humidity up to 58 meters.

Index Terms—Batteryless sensors, Chipless sensors, Direction-of-Arrival analysis, Flexible electronics, Internet of Things, Microstrip antenna arrays, Antennas arrays, Radar imaging, Remote sensing, RFID sensors

I. INTRODUCTION

WITH the explosion of active electronic devices with integrated sensors, the remote reading of physical quantities is no more challenging in Internet of Things related applications. Nevertheless, the electromagnetic waves propagation, typically required for the wireless transmission of sensor data, imposes serious limitations in terms of the maximal range of interrogation, the multi-sensors interrogation capability, the embedded battery lifetime and the available frequency bandwidth. These constraints limit the applicability and the performance of wireless sensor network (WSN) technologies in numerous practical scenarios. WSN devices are often commercialized under different protocols of communication such as BLE (Bluetooth Low Energy), ZigBee

or LoRa [1]. Typically, the end nodes of these networks are active devices with integrated circuits and batteries that generate specific frames for communication. The battery lifetime of such sensors can last up to 10 years for specific configurations [2] and use cases. However, due to the active nature of the required circuitry, compounded by the mW power consumption levels of their transceivers during transmissions, such battery lifetimes can only be achieved at the cost of heavy duty cycling. Such operation is inappropriate for time-sensitive sensing and monitoring applications. Moreover the wireless measurement of physical quantities becomes especially challenging in harsh environment that limits the amount of human intervention, such as very high or very low temperature and pressure, or even radioactivity. Hence, continuously interrogated sensors with long lifetime and long achievable range are highly required. One possible solution is the use of remotely readable passive sensors (without integrated devices and DC power supply) because their lifetime depends only on their constitutive material properties. However, the main technical challenge lies in deriving the physical quantity of interest from the measurement of sensors' electromagnetic echoes at a very long interrogation range.

Several technologies are currently used to perform effectively the remote interrogation of passive sensors. Radio-Frequency Identification (RFID) technology is widely utilized in many applications for both tag identification (based on a barcode reading) and tag sensing. However, power regulations do not allow RFID's to achieve a sufficient interrogation range (typically < 10 meters) in applications where environments are harsh and highly reflective (note that Surface Acoustic Wave sensor interrogation has been demonstrated in [3] for range up to 30 meters in specific configurations). In addition, working at low frequencies can be problematic for the integration of small antennas. Moreover the electromagnetic to acoustic wave transitions can further degrade the range of interrogation. Other technologies at higher frequencies exist, such as passive millimeter-wave identification (MMID) sensors working around 60 GHz, allowing the miniaturization of passive tags, like pressure sensors [4], and featuring a range of interrogation of only few meters.

This paper is originally based on a previous version which

Manuscript received June 30, 2017. This paper is an expanded version from the 2017 International Microwave Conference, Honolulu, HI, 4–9 June 2017.

This work was supported in part by the French Technological Research Agency, Ovalie-Innovation, Occitanie Region (CARANUC project) and by H2020-ICT (DOSIRA-GATEONE project).

D.Henry, H.Aubert and P.Pons are with LAAS-CNRS, Toulouse, 31031 France (+33 561 336 930; e-mail: dhenry@laas.fr).

J.Hester and M.Tentzeris are with School of Electrical and Computer Engineering, Georgia Institute of Technology, Atlanta, Ga 30332.

proposes for the first time an alternative technique to the standard RFID interrogation in order to locate and remotely read flexible passive humidity sensors at long interrogation ranges (>50 m) [5]. The present extension reports the more detailed description of three different beam scanning techniques, including the Synthetic Aperture Radar (SAR) beam scanning approach. Moreover, an enhanced estimation of the humidity is proposed here from adding additional contributions to the measured echo level distribution, and by improving the linearity of the long-range relative humidity estimation. Finally, it is shown that the relative humidity at the sensor location can be derived from the proposed beam scanning techniques even if undesirable clutters are present inside the volume of analysis. The sensor tag can be used to monitor the humidity on targeted areas with difficult access, and avoids battery replacement in structural health monitoring applications. The obtained long-range interrogation enlightens all the potential of such passive tags and the proposed method of interrogation can be extended to the wireless measurement of various physical or chemical quantities using Van-Atta reflectarray sensors.

The proposed technique merges technologies from two different domains: (a) a Frequency-Modulated Continuous-Wave (FMCW) scanning method involving signal processing, Synthetic Aperture Radar (SAR) and statistical estimators, and (b) the design of passive sensors using humidity-sensitive Kapton-based Van-Atta retrodirective arrays. This original technique was already introduced in [6], [7] although there was no report of its use for an integrated passive sensor and, at such a long distance and with the measurement sensitivity reported here. The sensitivity improvement is mainly due to the combination of the cross-polarization and retrodirective effects of the reflectarray which enhances the Signal-to-Noise-Ratio (SNR). Moreover, this kind of humidity passive sensors was wirelessly interrogated at only 5.5 meters [8] and detected at 30.0 m [9]. Such results require at least a 4 GHz frequency band (13%) around 30 GHz to perform the required full-scale dynamic range measurement.

The first part of the paper describes the hardware used for the interrogation technique as well as the properties of the Van-Atta reflect array. Three mechanical beam scanning techniques are described in detail here for the remote estimation of the relative humidity with high accuracy: (a) the spherical beam sweeping performed by a stationary radar, (b) the cylindrical beam sweeping performed also by a stationary radar and (c) the SAR obtained from the uniform linear motion of the radar with constant velocity. The second part is focused on the indoor interrogation of the humidity passive sensors at different ranges of interrogation up to 58.0 meters. Several methods are investigated in order to achieve the largest full-scale measurement range and the highest linearity. Special attention will be devoted to the definitions of statistical estimators from the Gaussian distribution of measured electromagnetic echoes and linearity corrections. A three-dimensional display of echoes using convenient isosurfaces is

also reported with/without the presence of passive humidity sensors in a highly cluttered environment. Measurement results obtained from the remote reading of the Van-Atta reflectarray at different angles of incidence are finally discussed and a direction-of-arrival (DoA) analysis is applied to remove undesirable echoes.

II. WIRELESS INTERROGATION OF PASSIVE SENSORS

This chapter focuses on the hardware description of the reader (24GHz FM-CW radar mounted on a mechanical platform) and the passive humidity sensor (Van-Atta sensor reflectarray).

A. Radar Beam Scanning Description

The reader is often called *short-range* FM-CW radar [10] because it allows targets detection below 100 meters. However it is actually a *long-range* reader when used for the wireless interrogation of passive sensors as it allows reading range above 5 meters. More specifically it is demonstrated here that reading ranges of passive sensors up to 58 meters are possible [5].

The 24GHz FM-CW radar from IMST GmbH (DK-sR-1030e model) transmits a so-called *chirp* that is a triangular frequency modulated signal. In our proof-of-concept demonstration, the carrier frequency is of 23.8 GHz. This choice brings many advantages, such as: (a) a good achievable linearity of the radar voltage control oscillator over a wide frequency band ($B=2$ GHz), which is mandatory for ensuring a sufficient depth resolution d ($d=c/2B=7.5$ cm, where c denotes the velocity of light [11]); (b) an operating frequency in the ISM band and (c) the design of small size passive sensors with integrated miniaturized antennas. The duration T of the up-ramp of the modulation is 5ms and corresponds to a chirp rate B/T of 0.4 GHz.ms⁻¹. Note that the frequency band B used here exceeds the ISM band limits of 250 MHz. However it has already been shown in [6] that it is possible to interrogate passive sensors in such narrower bandwidth, but at the expense of degradation in measurement sensitivity.

A mechanical beam scanning is performed as the transmitted (Tx) channel of the FMCW radar is connected to a rotating parabolic antenna with the gain of 33.5 dBi and the 3 dB beamwidth of 2° . The rotation has a step of 1° in azimuth and elevation. The mechanical pan-tilt (Pelco PT570P) is synchronized with the transmitted signal through a computer unit. The electromagnetic signals backscattered by the sensors are received (Rx) by two arrays of 1×5 patch antennas separated by the half-wavelength of the carrier frequency (6mm). This separation distance allows deriving the directions of arrival of backscattered signals. The gain of the Rx-antenna is of 8.6 dBi and the beamwidths of this antenna are of 60° and 25° in azimuth and elevation, respectively. The Tx and Rx antennas are also positioned in orthogonal linear polarizations, in order to take advantage of the cross-polarizing properties of the printed Van-Atta humidity sensor. A spatial translation of the radar system is also performed. Let $df=2D^2/\lambda$ be the Fraunhofer distance, where $D=50$ cm is the largest antenna

dimension of the parabolic dish diameter. Consequently, the theoretical separation distance between far and near field regions stands at $df=39.6$ m. The radar output power is 20 dBm (100 mW).

This platform is used here for comparing the performances of three possible mechanical beam scanning techniques for the remote interrogation of passive humidity sensors, that is, (a) the spherical beam sweeping and (b) cylindrical beam sweeping performed by a stationary radar and, (c) the SAR-type scanning obtained from the uniform linear motion of the radar with constant velocity.

The electronic beam scanning could be used instead of the proposed mechanical scanning. However the mechanical beam scanning offers the advantage to perform accurate rotations both in azimuth and elevation, and contrary to the electronic scanning using fixed (static) antennas, it ensures the same beamwidth (i.e., the same angular resolution) in all beam directions, as Tx and Rx-antennas keep unchanged their beamwidth during the rotation.

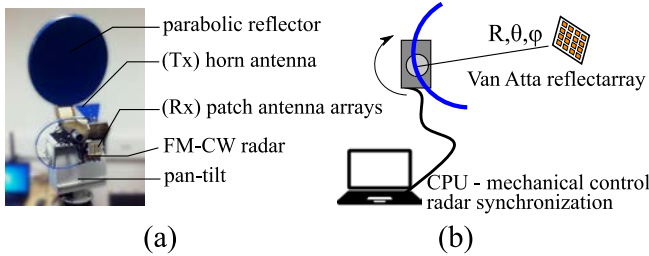


Fig. 1. (a) FM-CW radar interrogation system. Tx and Rx antennas have orthogonal linear polarizations to take advantage of the cross-polarization effect of the relative humidity passive sensor. The mechanical beam scanning in azimuth and elevation is performed using a pan-tilt. [5] (b) The pan-tilt and radar system are synchronized to perform the beam scanning.

B. Kapton-based Van-Atta passive humidity sensors

The proof-of-concept passive humidity sensor used for the measurements is a 74×74 mm² Van-Atta reflectarray structure (see Fig. 2(a)). It is composed of five side-by-side linear antenna arrays and inkjet-printed on an easily low-cost and integrable flexible substrate (Kapton HN polyimide). It has the property to retransmit the incident waves in phase and in cross polarization. The linear antenna arrays of the tag are connected following the characteristic Van-Atta scheme. Contrary to basic Van-Atta reflect-arrays, two connecting networks are here required in the structure, in order to connect both complementary polarization couples and thereby inducing a cross-polarization of the re-emitted signal. As reported in [8] and [9], such flexible printed Van-Atta targets provide a simultaneously high and largely isotropic radar cross-section (RCS) that is, in addition, extremely robust to bending. These combined properties confer high detectability from a large range of incident angles, as well as enable conformal mounting and polarimetric detection compatibility. Using the bistationary FM-CW radar for the linearly polarized incident electromagnetic fields facilitates the detection of the passive sensor by increasing the Signal-to-Noise Ratio (SNR). Moreover the sensor ground plane allows the placement of the

sensor in close proximity of metallic clutter without degrading its re-radiating properties.

The permittivity of the Kapton is very sensitive to humidity of which a small change generates an observable shift of the device resonant frequency [9]. According to the substrate datasheet, the relative permittivity of the used Kapton is a function of relative humidity (RH) as follows: $\epsilon_r = 3 + 0.008RH$.

Thus, an appropriately designed passive sensor at 24 GHz provides a measurable echo level fluctuation. To demonstrate the unique properties of the proposed reflectarray-based sensor wireless, indoor measurements of this sensor are performed in a long (60 meters) corridor (Fig. 2(b)). In comparison with outdoor or non-reflective environments, performing indoor measurement may generate significant multipath and decrease the SNR. This is generally due to high reflective cluttering objects, such as metallic grids or walls. It was intended to perform these measurements in such conditions to validate the experiment in a non-ideal rugged environment.

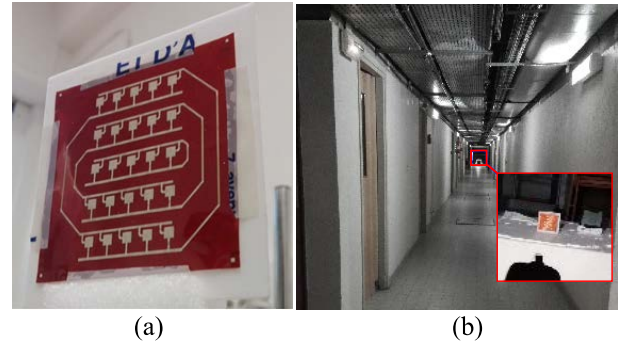


Fig. 2. (a) Kapton-based Van-Atta reflectarray prototype and (b) long range (60 meters) and indoor remote measurement setup of this prototype in a corridor. [5]

III. MEASUREMENT RESULTS AND DISCUSSION

Different methods are detailed in this Section to measure the relative humidity from the wireless interrogation of Van-Atta reflectarray. In Section III.A the structure of the multidimensional radar data grid for three mechanical beam scanning techniques (reported as solutions n°1, n°2 and n°3) is described. The solution n°1 (spherical sweeping) is then applied in Section III.B to interrogate the Van-Atta sensor reflectarray located at 1.3 meter from the reader. Several estimators are derived to retrieve the relative humidity. In section III.C, solutions n°1 and n°2 are combined to perform the so-called *sweeping combination*. This beam scanning is applied for the wireless reading of a sensor reflectarray located at 10 meters from the reader. In Section III.D the solution n°3 (SAR beam scanning) is reported. Measurement results for these different beam scanning techniques are reported in Table 1. In Section III.E the feasibility of interrogating Van Atta sensor reflectarray at long ranges of interrogation (up to 58 meters) is demonstrated.

A. Passive sensor remote interrogation using three different multi-dimensional radar beam scanings

The main principle of the multi-dimensional radar beam

scanning (2D or 3D) is to analyze the signals backscattered by the passive sensor when using multiple directions of interrogation. Several beat frequency spectra (that is, one spectrum per direction of interrogation) are then obtained from the 3D scanning, and processed in a volume of analysis composed of so-called *voxels* (When a 2D scanning instead of a 3D scanning is used, beat frequency spectra are processed on a surface of analysis composed of so-called *pixels*). To each voxel, a specific echo level is assigned and is expected to contain some information on the humidity at the passive sensor location.

Three mechanical beam scanings are considered here for the remote estimation of the relative humidity: (a) the spherical beam sweeping performed by a stationary radar (solution n°1), (b) the cylindrical beam sweeping performed by a stationary radar (solution n°2) and, (c) the SAR-type scanning obtained from the uniform linear motion of the radar with constant velocity (solution n°3). Each of these three scanings generates a specific voxel volume or surface which characterized the spatial resolution of the chosen scanning. The volume resolutions V_S (solution n°1) and V_C (solution n°2), and the surface resolution S_{SAR} (solution n°3) are given by:

$$V_S = \left(2R^2 d + \frac{d^3}{6} \right) \cdot \theta_s \cdot \sin\left(\frac{\varphi_s}{2}\right) \quad (1)$$

$$V_C = R \cdot d \cdot d_x \cdot \varphi_s \quad (2)$$

$$S_{SAR} = d \cdot v \cdot PRI \quad (3)$$

where R denotes the distance between the center of the voxel and the radar while θ_s , φ_s and d_x designate the steps in azimuth, elevation and cross-range, respectively; d is the previously defined depth resolution (see Section II.A); v is the constant velocity of the radar during its uniform linear motion; PRI is the pulse repetition interval of the radar. Equations (1)-(3) are valid here since the duty-cycle T/PRI of the FM-CW radar is low ($T/PRI=5\%$ for $PRI=100$ ms). The voxel volume for the 3 solutions considered here is illustrated in Fig. 3.

B. Indoor sensor interrogation at 1.3 meters and definition of statistical estimators of the relative humidity

Wireless measurements are first performed to study the linearity and the full-scale measurement range of the Van-Atta reflectarray humidity sensor. For this purpose the passive sensor is placed in a homemade chamber with a humidity controller and a reference humidity sensor (Fisherbrand 90954) with an accuracy of $\pm 5\%$.

The chamber has a very low relative permittivity (ϵ_r very close to 1) to minimize electromagnetic reflections. The ambient humidity inside the chamber increases by heating a humid sponge. The relative humidity and the temperature are recorded at the beginning and at the end of each measurement.

For this very first experiment the distance between the radar and the sensor is set at 1.3 meters. The spherical sweeping (solution n°1) is chosen with an angle of $\pm 10^\circ$ in azimuth and

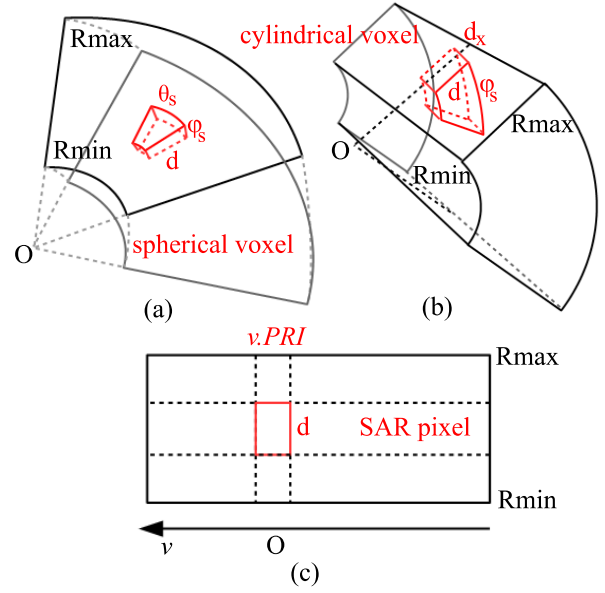


Fig. 3. Voxel generated by: (a) the spherical beam sweeping by a stationary radar, (b) the cylindrical beam sweeping performed by a stationary radar and (c) the SAR-type scanning obtained from the uniform linear motion of the radar with constant velocity v . The point O represents the radar position.

$\pm 10^\circ$ in elevation requiring the recording of 441 beat frequency spectra (about 3960 voxels) at different interrogation directions.

The relative humidity can be remotely derived from the calculation of statistical estimators. The estimator can be defined as the echo level of specific voxel or as the combination of echo levels at different voxels.

When defining a statistical estimator of the humidity from the analysis of the 3D (or 2D) radar image, four key parameters must be considered: the achievable dynamic range D of the estimator; the sensitivity η of the estimator with respect to humidity; the linearity of the estimator with respect to humidity (this linearity is characterized by the coefficient of determination R^2); and finally the standard error or precision ϵ , that is, the difference between the value of the estimator and the value given by the linear regression of the estimator with respect to humidity.

Three statistical estimators are proposed here to derive the relative humidity from the measured scattering data:

- The value e_{Max} of the – unique – voxel containing the maximal echo level.
- The mean echo level e_A of all voxels values in the total interrogated volume.
- The estimator e_S such that $s=\phi(e_S)$ where s is a given number of voxels and ϕ denotes *Gaussian-like* distribution of the measured echo level. This function is given by:

$$\left\{ \begin{array}{l} \phi(x) = \frac{K}{\sigma} \cdot G\left(\frac{x-\mu}{\sigma\sqrt{2}}\right) \cdot \Phi\left(\alpha \cdot \frac{x-\mu}{\sigma}\right) \\ \text{with } G(x) = \frac{\exp(-x^2)}{\sqrt{2\pi}} \\ \text{and } \Phi(x) = \frac{1}{2} \left(1 + \operatorname{erf}\left(\frac{x}{\sqrt{2}}\right) \right) \end{array} \right. \quad (4)$$

where K is the scaling factor, μ denotes the shift (in dB) of the distribution, σ designates the standard deviation and erf is the error function. Compared with our earlier work [5], the probability density function (PDF) has been modified by defining the domain of ϕ in dB scale and by adding the contribution of the function Φ , which generates an asymmetry controlled by the skewness parameter α [12]. This asymmetry allows improving the fitting of the PDF to the measurement results and then deriving a more accurate description of the echo level distribution. Measurement results are fitted to ϕ for given values of the parameters μ , σ , K and α , followed by a Kolmogorov-Smirnov test [13] between the PDF and the measurement data. The Kolmogorov-Smirnov test can be applied here if the parameters of the distribution are correctly defined. If the resulting two-tailed p-value of the test is lower than 95%, the echo level interval is reduced and ends to a success test with $p \geq 95\%$. The sensitivity of this test is often higher at the center of the distribution where the impacts on the tails of the distribution are limited. For a better sensitivity of this test at the tails of the distribution (i.e., for high echo levels or for noise echo levels), the Anderson-Darling [14] test could be preferred.

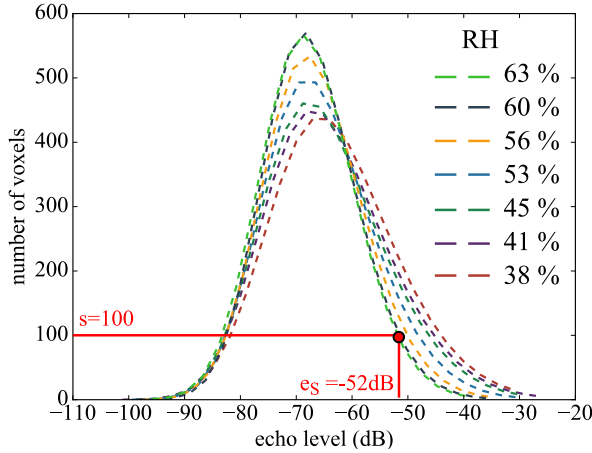


Fig. 4. Measured *Gaussian-like* distribution of the echo level for various relative humidity using the Van-Atta reflectarray humidity sensor interrogated at 1.3 meters. From this statistical distribution, the estimator e_S is computed for a given number of voxels. As indicated in the figure, for a relative humidity 63% and $s=100$ voxels, the estimator e_S is found to be of -52dB.

To enlighten the physical meaning of the statistical estimator e_S , the distribution ϕ is plotted in Fig. 4 for various relative humidity. It can be observed that the profile of the distribution varies with RH . As RH changes the estimator e_S varies, and depends on the number s of voxels: a small number of voxels (including extrapolating values inferior to 1) leads to high dynamic range D at the expense of low measurement precision ε . The requirement for optimal value of s (if exists) could be a precision from e_S close to one obtained from e_{Max} and a sensitivity of e_S better than one achieved by e_{Max} .

The three estimators e_{Max} , e_A and e_S are computed for RH varying from 38% to 69% (see Fig. 5). The resulting key above-defined parameters D , η , R^2 and ε of these estimators are reported on Table I. Here $s=4$ voxels which leads to a

sensitivity (0.6 dB/%) higher than e_{Max} (0.4 dB/%). In order to improve the precision (ε) and the linearity (R^2) of the estimator e_S , a correction is applied based on the high linearity of the estimator e_A . To apply this correction, let a_A and a_S be the sensitivities with respect to relative humidity RH of estimators e_A and e_S , respectively. Moreover let b_A and b_S the intercepts (estimator value for $RH=0\%$) of linear regressions of the estimators e_A and e_S , respectively. As a consequence, it can be written that $e_A = a_A \cdot RH + b_A$ and $e_S = a_S \cdot RH + b_S$. For $RH > 50\%$, the correction consists of computing the following estimator:

$$e_{SC} = \frac{a_S}{a_A} (e_A - b_A) + b_S \quad (5)$$

From this estimator the RH is obtained with a better precision (0.7 dB instead of 0.9 dB) and an improved linearity ($R^2=0.98$). Consequently, the analysis of statistical estimators like e_S offers many advantages as it allows improving the sensitivity of the passive sensor by at least 50% without impacting the measurement precision.

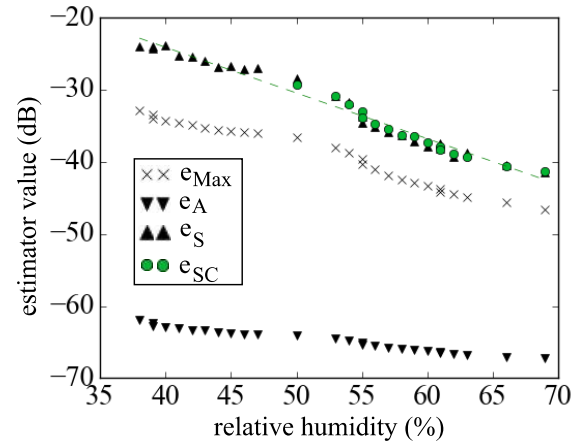


Fig. 5. Statistical estimators e_{Max} , e_A , e_S and e_{SC} (see text) as a function of relative humidity using the Van-Atta reflectarray humidity sensor interrogated at 1.3 meters. A correction (green dots) is applied on the estimator e_S ($s=4$ voxels) by taking advantage of the linear behavior of the estimator e_A .

C. Indoor interrogation at 10.0m and sweeping combination method

When performing the spherical beam sweeping with a stationary radar (solution n°1), the volume of the voxel increases with distance R (see (1)). From (2), a cylindrical sweeping (solution n°2) can be used to reduce the voxel volume. However the challenge is to retrieve the voxel of highest echo when the position of the sensor is not accurately known at long interrogation ranges. For the sake of illustration the Van-Atta reflectarray humidity sensor is placed at 10.0 meters from the radar. A spherical sweeping (solution n°1) is performed with an angle of $\pm 5^\circ$ in azimuth and $\pm 5^\circ$ in elevation, generating a volume containing 270 voxels. Fig. 6 is the resulting three-dimensional (3D) representation of the ambient echo level at distances (z-direction) between 10.0 meters and 10.2 meters for $RH=34\%$. It is displayed with isosurfaces [15] (layers of same echo level) which are

superimposed on a 3D Cartesian grid. Inside the volume are included the echo levels of interest but also spurious echoes (clutters). If the clutter is not removed, the humidity estimation is erroneously obtained from the estimator called e_{MaxERR} . Nevertheless the clutter can be ignored by focusing the analysis on echoes of a small volume incorporating the sensor. In this case a second estimator is extracted, called here e_{MaxOPT} . However this estimation requires knowing the exact position of the sensor (or in another perspective the exact position of the radar). Another solution consists of performing a step-by-step linear translation of the radar (perpendicular to the direction of interrogation) after each spherical sweeping. This method (combination of solutions $n^{\circ}1$ and $n^{\circ}2$) is called here the *sweeping combination* as it is equivalent to combine data from cylindrical and spherical sweepings. From solutions $n^{\circ}1$ and $n^{\circ}2$ and the resulting probability density function defined in Eq.(4), the new statistical estimator $e_S(n)$ is computed, where n designates the number of linear steps ($n=0$ corresponds to solution $n^{\circ}1$). For illustration purpose, five spherical sweepings separated by a step d_x of 1 cm are performed. Compared to solution $n^{\circ}1$, 5 times more voxels are registered in each beam direction. Moreover, the second Rx channel is used in order to take into account the echoes of around 2700 voxels.

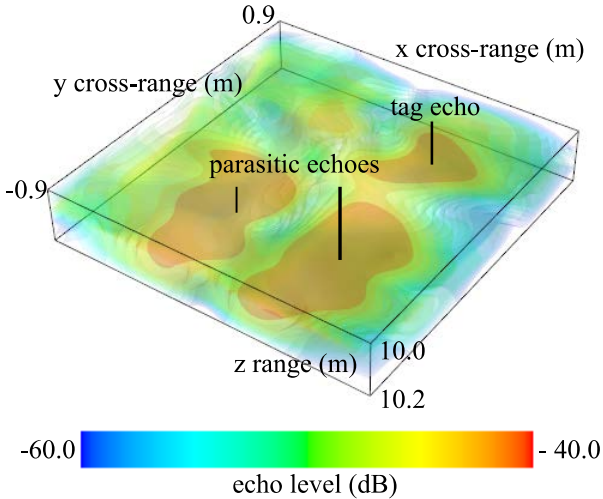


Fig. 6. 3D echo level of the scene at a range R between 10.0 meters and 10.2 meters. It includes the echo response of the tag for $RH=37\%$ as well as parasitic echoes (clutters)

The statistical estimators e_S (with $s=4$ voxels), e_{MaxERR} , e_{MaxOPT} and $e_S(n=4)$ are displayed in Fig. 7 for a relative humidity varying from 34% to 74%. As expected, e_{MaxERR} is biased by spurious echoes which have a constant echo level around -33dB. If the sensor position is known, e_{MaxOPT} offers good performances with high linearity ($R^2=0.97$) and a full-scale dynamic range of 9.5 dB. If the sensor position is unknown, undesirable effects of clutters are attenuated as shown by $e_S(n=4)$ performances. The sensor echo variation is retrieved with a good linearity ($R^2=0.93$) and a precision ε of 1.5 %. These results are of course degraded in comparison with ones obtained from the estimator e_{MaxOPT} . However, the fact that the sensor echo level variation is detectable among higher echo levels is remarkable. The impact of the number of

steps adopted in solutions $n^{\circ}1$ and $n^{\circ}2$ (sweeping combination) can be observed in Table I. As expected, for the solution $n^{\circ}1$ only (spherical sweeping) the relative humidity estimation is not as good as for the combined solutions with $n \geq 1$ ($R^2=0.88$ and $\varepsilon=5.0\%$). This is due to a less number of voxels and informative echo data in solution $n^{\circ}1$ only compared to solutions $n^{\circ}1$ and $n^{\circ}2$ combined.

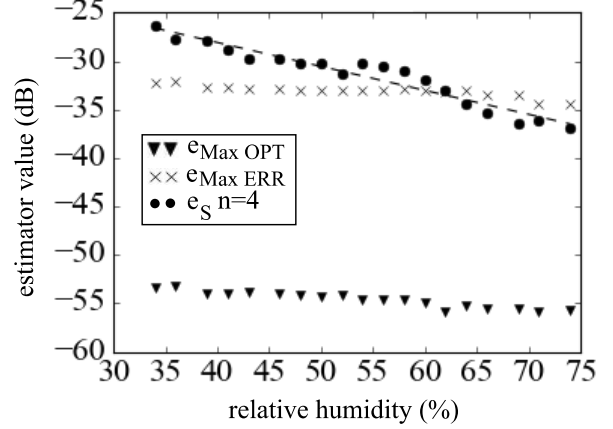


Fig. 7. Statistical estimators e_{MaxOPT} , e_{MaxERR} and $e_S(n=4)$ (see text) as a function of relative humidity using the Van-Atta reflectarray humidity sensor interrogated at 10.0 meters. The estimator $e_S(n=4)$ computed from the sweeping combination solution $n^{\circ}4$ allows retrieving the sensor echo variation despite the high level of parasitic echoes, embedded in the estimator e_{MaxERR} .

D. Remote reading of humidity sensor at 2.1 meters using a SAR beam scanning

For this experiment, the Van-Atta reflectarray humidity sensor is placed on a conveyor belt at a distance of 2.1 meters from the radar. The passive sensor has a constant speed $v=3.8$ $\text{cm}\cdot\text{s}^{-1}$ and the radar system is stationary, as depicted in Fig. 8 (a). This configuration is equivalent to solution $n^{\circ}3$ (SAR scanning) introduced in Section II.A in which the humidity sensor is stationary and is interrogated by a radar having a uniform linear motion with constant velocity of $v=3.8$ $\text{cm}\cdot\text{s}^{-1}$.

The pulse repetition interval PRI of the radar is of 100 ms and leads to a duty cycle T/PRI of 5%. From the radar and antenna parameters, the stop-and-go approximation can be used and Doppler shift effects can be neglected [16]. The 2D radar data grid is then generated by applying a FFT on the time signal at each PRI (Fig.8 (b)). Two-dimensional radar images for different values of relative humidity are displayed on Fig. 9. In this Figure the ordinate is the interrogation range (theoretical resolution d of 7.5 cm) while the abscissa is the cross-range (resolution d_x of 3.8 cm with a PRI of 100 ms). The echo levels at distances close to 2.1 m are mainly due to the sensor backscattering and depend on the relative humidity. For $RH=20\%$ the sensor backscattering is maximal and is associated to the highest echo level. For $RH=56\%$, the resonant frequency of the reflectarray is found to be out of the frequency band of the radar. Consequently a low echo level is measured. Additional high echoes can be observed at 3 meters and are the constant clutters from the environment. These undesirable echoes must not be taken into account in the

estimation of the relative humidity. From Eq.(3), the surface resolution S_{SAR} is here of 28.5 cm^2 . This resolution depends on speed v of the sensor when using stationary radar (or of the radar velocity when interrogating stationary sensor) and on the PRI . The estimator e_{Max} is reported on Table I for different values of PRI . It has been calculated for a relative humidity varying from 20% to 56%. A good linearity ($R^2=0.99$) and precision (1.0 dB) of e_{Max} is obtained with a dynamic range of 9.0 dB. As expected, both the linearity and precision are degraded when the PRI exceeds 1 second.

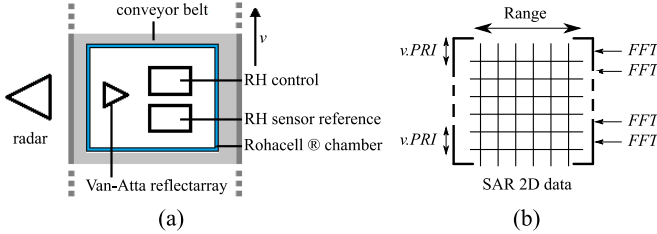


Fig. 8. (a) Van-Atta reflectarray humidity sensor placed on a conveyor belt at a distance and interrogated by a stationary radar. An equivalent configuration would consist of interrogating a stationary sensor by a radar having a uniform linear motion with constant velocity. The passive humidity sensor is located at 2.1 m from the radar and the conveyor speed is of 3.8 cm.s^{-1} . (b) Generated 2D SAR data grid.

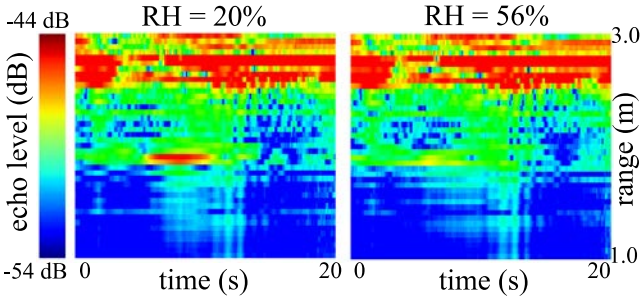


Fig. 9. Two-dimensional display of the electromagnetic echo of Van-Atta reflectarray humidity sensor echo located at 2.1m in front of the radar, for $RH=20\%$ (left) and $RH=56\%$ (right). High echoes observed at 3 meters are due to surrounding clutters.

From all the results reported in Table I, it can be observed that the estimators performance depend on the reading range: more the tag is close to the radar more the sensitivity is raised (the sensitivity reaches $0.6 \text{ dB}/\%$ at 1.3 meters. This is due to a degradation of the SNR as the reading range increases. Nevertheless the relative humidity can be derived from a calibration process and link budget. Independently of the interrogation range, the accuracy of the proposed estimators can be improved. For the sweeping combination (solutions $n^{\circ}1$ and $n^{\circ}2$), the linearity (R^2) increased with the number of translations ($n=4$). Moreover, for the SAR beam scanning (solution $n^{\circ}3$), the sensitivity and linearity are enhanced from reducing the PRI of the radar (or equivalently, from generating finer radar data grids).

E. Long range radar interrogation (58 meters) of the passive humidity sensor and DoA analysis

The Van-Atta humidity sensor reflectarray is now located at 58.0 meters from the radar and for a relative humidity of 48%. A picture of the experimental setup is shown in Fig. 2(b). Due to hardware limitations, only $N=1024$ samples are used here for discretizing the chirp up-ramp frequency modulation. As a consequence, it is no more possible at this distance to perform echoes measurement with the radar bandwidth of 2 GHz. The bandwidth can be set to 1.2 GHz leading to a lower theoretical depth resolution ($d=12,5 \text{ cm}$) and a theoretical maximal interrogation range of $d \times N/2=64$ meters. Moreover, the x-range and y-range resolutions are found to be of 1.0 meter for the adopted 1° mechanical sweep step. Fig. 10 displays the three-dimensional representation of the ambient echo (clutter) level at distances (z-direction) between 57.5 meters and 58.5 meters. The estimator e_{Max} (that is, the value of highest echo magnitude in the volume of analysis) for the passive sensor echo levels over the isosurfaces found to be of -56.2 dB . The Van-Atta reflectarray humidity sensor is visible among the clutter with a dynamic range difference of 6 dB, knowing that the maximal echo from the clutter is $e_{Max}=-62.1 \text{ dB}$. This difference of 6 dB has been measured by analyzing e_{Max} with and without the reflectarray. Despite the lower depth and cross-range resolutions, it is very encouraging to observe that the echo level of the clutter is very small compared with the echo of the humidity sensor at such long distances. If the sensitivity of $0.2 \text{ dB}/\%$ is preserved, the full-scale dynamic range (which is the echo level difference between the highest and lowest echo levels generated by the reflectarray) is close to 9 dB. This long range indoor interrogation is possible by using the cross-polarization effect of the reflectarray: the depolarization effect becomes a discriminant criterion because

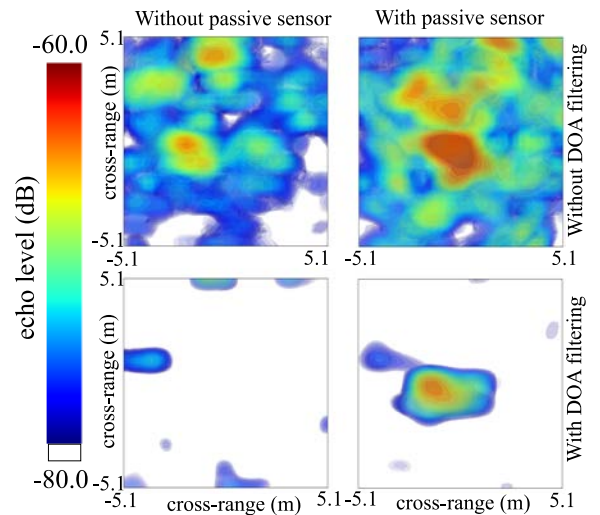


Fig. 10. 2D echo level of the scene at a range R between 57.5 m and 58.5 m with (right) and without (left) the passive humidity sensor. A picture of the experimental setup is shown in Fig. 2(b). Due to the cross-polarization effect, the sensor is detectable at these long distances. A Direction-of-Arrival filter (bottom) removes the undesirable echoes (clutter) and the multi-path generated by the walls of corridor.

it was observed that the environment depolarizes significantly less than the passive sensor.

To illustrate the impact of the radar position and of the corridor on the long-range remote derivation of the relative humidity, the estimator e_{Max} is now calculated for different beam directions and different linear shifts by performing a sweeping combination (solutions n°1 and n°2). The electromagnetic signals backscattered by the sensor are received (Rx) by two antenna arrays (Antenna 1 and Antenna 2) of 1x5 patch antennas separated by a distance of 6mm with the gain of 8.6 dBi and the beamwidth of 60° and 25° in azimuth and elevation, respectively. Results are shown on Fig. 11 for the two antennas arrays. It can be observed that the echo level difference between the two reception channels at the same position is of 10 dB in Fig. 11(a). These differences may originate in the retrodirective effect of the Van-Atta reflectarray, which reflects the signal at a specific angle. Since the DoA is not equal to 0°, a difference of echo levels occurs. It enlightens the fact that, for long interrogation range of sensor in environments such like corridors, the beam direction

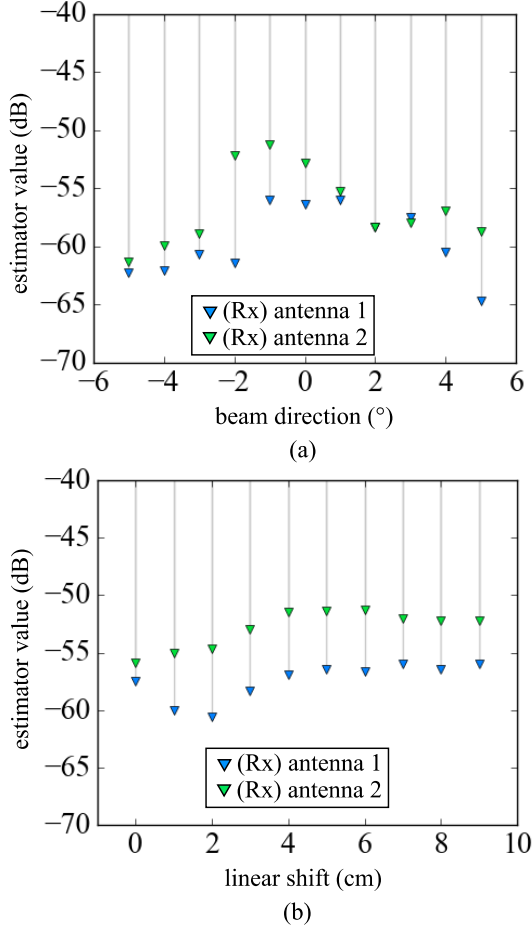


Fig. 11. Humidity estimator e_{Max} computed from the measured electromagnetic echoes of a passive sensor located at 58.0 meters from the radar as a function of: (a) different beam directions with a cylindrical sweeping (solution n°2) and (b) different cross-range positions with a spherical sweeping (solution n°1). The backscattered signal is received by two antenna arrays (Antenna 1 and Antenna 2) of 1x5 patch antennas separated by a distance of 6mm with the gain of 8.6dBi and the beamwidth of 60° and 25° in azimuth and elevation, respectively.

of the transmitting antenna has to be controlled with high accuracy ($< 1^\circ$) for appropriately interrogating Van-Atta reflectarray sensors. This angle-dependent critical issue can be avoided from performing a beam scanning. Moreover there is an echo level difference up to 10 dB between two different positions for the common reception channel in Fig11. (b). It means that the corridor generates multipath propagation and a non-zero azimuthal DoA. The DoA analysis can discriminate the passive sensor echo from undesirable echoes from the clutter. The standard 2D MUSIC algorithm [17] is used here. The algorithm (not detailed here) assigns a DoA value to each voxel of the radar data grid. A spatial filter is applied to reduce the voxels contribution for which the DoA is higher than -5° . Results are shown on the bottom of Fig. 10. Only the echoes generated by the Van-Atta reflectarray humidity sensor emerge from the 2D display and the clutter is no more apparent. The DoA analysis is consequently an efficient tool for removing the unwanted echoes (clutter) when interrogating passive sensors at long distance.

IV. CONCLUSION

This article has reported in details different configurations to interrogate passive sensors with a FMCW radar and to obtain the high linearity and dynamic measurement range. For this purpose, a Van-Atta reflectarray humidity was used as a passive humidity sensor. The analysis of a multidimensional electromagnetic echo response is explored from three types of beam scanning techniques: a spherical sweeping, a cylindrical sweeping and a SAR-type scanning obtained from the uniform linear motion of the radar with constant velocity. Statistical estimators of the humidity are defined for the remote derivation of relative humidity from radar echoes. For a sufficient number of voxels, the full-scale dynamic range of 17 dB is obtained with a measurement sensitivity of 0.6 dB/%. By using a method called the *sweeping combination*, it is possible to estimate the relative humidity among high level of parasitic echoes without knowing the exact position of the passive sensor. For industrial applications, the on-fly measurement of moving passive sensors (uniform linear motion of the radar with constant velocity) is demonstrated at a distance of 2.1 meters from the stationary radar: a sensitivity of 0.3 dB/% is obtained in this case. Finally, thanks to its cross-polarization effect, the Van-Atta reflectarray humidity sensor is detected at the unprecedented long distance of 58.0 m for different radar positions in an indoor environment (corridor). It was shown that multipath propagation and clutter impact may be removed from applying the Direction-of-Arrival analysis to passive sensors echoes.

The next steps are now to explore the limits of the proposed 3D active remote sensing technique in terms of resolution, precision and maximal distance of interrogation, as well as multi-sensors capabilities.

TABLE I
ESTIMATORS PARAMETERS

Spherical beam sweeping performed by a stationary radar (solution n°1) Interrogation range : 1.3m				
estimator for RH [38%-69%]	D (dB)	η (dB/ %)	R^2	ε (%)
e_{Max}	13.7	-0.4	0.97	1.7
e_A	4.7	-0.1	0.98	2.0
$e_S (s=4)$	17.0	-0.6	0.97	1.5
$e_S Corrected$	17.0	-0.6	0.98	1.1
Sweeping combination (combination of solutions n°1 and n°2) – Interrogation range : 10.0m				
estimator for RH [34%-74%]	D (dB)	η (dB/ %)	R^2	ε (%)
$e_{Max Opt} - without clutter$	9.5	-0.2	0.97	2.5
$e_S (n=4, s=4) - with clutter$	10.5	-0.2	0.93	4.0
$e_S (n=3, s=4) - with clutter$	10.6	-0.2	0.93	4.0
$e_S (n=2, s=4) - with clutter$	10.0	-0.2	0.93	4.0
$e_S (n=1, s=4) - with clutter$	10.9	-0.2	0.92	4.5
$e_S (n=0, s=4) - with clutter$	10.3	-0.2	0.88	5.0
SAR-type scanning obtained from the uniform linear motion of the radar with constant velocity (solution n°3) – Interrogation range : 2.1m				
estimator for RH [20%-56%]	D (dB)	η (dB/ %)	R^2	ε (%)
$e_{Max} - PRI = 0.1$ s	9.0	-0.3	0.99	1.0
$e_{Max} - PRI = 1.0$ s	9.4	-0.2	0.98	2.0
$e_{Max} - PRI = 2.5$ s	10.5	-0.2	0.94	2.5
$e_{Max} - PRI = 3.0$ s	10.5	-0.2	0.86	6.0

D: dynamic range for the given RH range.

η : sensitivity

R^2 : linearity or coefficient of determination.

ε : standard error or precision between the linear model and measurements

REFERENCES

- [1] A. J. Wixted, P. Kinnaird, H. Larijani, A. Tait, A. Ahmadinia and N. Strachan, "Evaluation of LoRa and LoRaWAN for wireless sensor networks," 2016 IEEE SENSORS, Orlando, FL, 2016, pp. 1-3. W.-K. Chen, Linear Networks and Systems (Book style). Belmont, CA: Wadsworth, 1993, pp. 123–135.
- [2] A. Dongare et al., "OpenChirp: A Low-Power Wide-Area Networking architecture," 2017 IEEE International Conference on Pervasive Computing and Communications Workshops (PerCom Workshops), Kona, Big Island, HI, USA, 2017, pp. 569-574.
- [3] D. C. Malocha, J. Humphries, J. A. Figueroa, M. Lamothe and A. Weeks, "915 MHz SAW wireless passive sensor system performance," 2016 IEEE International Ultrasonics Symposium (IUS), Tours, 2016, pp. 1-4.
- [4] D. Hotte, R. Siragusa, Y. Duroc and S. Tedjini, "A Concept of Pressure Sensor Based on Slotted Waveguide Antenna Array for Passive MMID Sensor Networks," in IEEE Sensors Journal, vol. 16, no. 14, pp. 5583-5587, July 15, 2016.
- [5] D. Henry, J.G.D Hester, H. Aubert, P. Pons and M.M. Tentzeris, "Long Range Wireless Interrogation of Passive Humidity Sensors using Van-Atta Cross-Polarization Effect and 3D Beam Scanning Analysis," 2017 IEEE MTT-S International Microwave Symposium (IMS), Honolulu, HI, 2017, under publication
- [6] D. Henry, H. Aubert and P. Pons, "3D scanning and sensing technique for the detection and remote reading of a passive temperature sensor," 2016 IEEE MTT-S International Microwave Symposium (IMS), San Francisco, CA, 2016, pp. 1-4.
- [7] D. Henry, H. Aubert and P. Pons, "Wireless passive sensors interrogation technique based on a three-dimensional analysis," 2016 46th European Microwave Conference (EuMC), London, 2016, pp. 49-52.
- [8] J. G. D. Hester and M. M. Tentzeris, "Inkjet-printed Van-Atta reflectarray sensors: A new paradigm for long-range chipless low cost ubiquitous Smart Skin sensors of the Internet of Things," 2016 IEEE MTT-S International Microwave Symposium (IMS), San Francisco, CA, 2016, pp. 1-4.
- [9] J. G. D. Hester; M. M. Tentzeris, "Inkjet-Printed Flexible mm-Wave Van-Atta Reflectarrays: A Solution for Ultralong-Range Dense Multitag and Multisensing Chipless RFID Implementations for IoT Smart Skins," in IEEE Transactions on Microwave Theory and Techniques, vol. PP, no. 99, pp. 1-11.
- [10] Boris A. Atayants, Viacheslav M. Davydochkin, Victor V. Ezerskiy, Valery S. Parshin and Sergey M. Smolskiy. "Precision FMCW Short-Range Radar for Industrial Applications", Artech House, 2014.
- [11] S. O. Piper, "Receiver frequency resolution for range resolution in homodyne FMCW radar," Conference Proceedings National Telesystems Conference 1993, Atlanta, GA, 1993, pp. 169-173.
- [12] Wahed, A.S., Ali, M.M.: "The skew-logistic distribution". J. Stat. Res. 35, 71–80 (2001)
- [13] Massey, F. J. "The Kolmogorov-Smirnov Test for Goodness of Fit." Journal of the American Statistical Association. Vol. 46, No. 253, 1951, pp. 68–78
- [14] Stephens, M. A. (1974). EDF Statistics for Goodness of Fit and Some Comparisons, *Journal of the American Statistical Association*, 69, pp. 730-737.
- [15] P. Ramachandran and G. Varoquaux, "Mayavi: 3D Visualization of Scientific Data," in Computing in Science & Engineering, vol. 13, no. 2, pp. 40-51, March-April 2011.
- [16] A. Meta, P. Hooeboom and L. P. Ligthart, "Signal Processing for FMCW SAR," in IEEE Transactions on Geoscience and Remote Sensing, vol. 45, no. 11, pp. 3519-3532, Nov. 2007.
- [17] F. Belfiori, W. van Rossum and P. Hooeboom, "Application of 2D MUSIC algorithm to range-azimuth FMCW radar data," 2012 9th European Radar Conference, Amsterdam, 2012, pp. 242-245.